

Melting heat transfer in the stagnation-point flow of third grade fluid past a stretching sheet with viscous dissipation

T. Hayat ^{a,b}, Z. Iqbal ^a, M. Mustafa ^{c,1} and Awatif A. Hendi ^b

^a Department of Mathematics, Quaid-I-Azam University 45320, Islamabad 44000, Pakistan

^b Department of Physics, Faculty of Science, King Saud University P. O. Box 1846, Riyadh 11321, Saudi Arabia

^c Research Centre for Modeling and Simulation (RCMS), National University of Sciences and Technology (NUST), Sector H-12, Islamabad 44000, Pakistan

An analysis has been carried out for the characteristics of melting heat transfer in the boundary layer flow of third grade fluid in a region of stagnation point past a stretching sheet. The relevant partial differential equations are reduced into ordinary differential system by suitable transformations. The series solutions are developed by homotopy analysis method (HAM). It is revealed that an increase in the melting parameter (M) decreases the velocity and the temperature (θ). An increase in the third grade parameter (ϕ) increases the velocity and the boundary layer thickness. The present results are also compared with the previous studies.

Keywords: Local similarity solution; Melting heat transfer; Stagnation-point flow; Third grade fluid; Boundary layer flow; Stretching sheet

1. Introduction

The boundary layer flows of non-Newtonian fluids have been widely recognized by the researchers in view of their immense technological and scientific applications such as polymer and food processing, oil recovery etc. In these fluids, the constitutive relationships between stress and rate of strain are much complicated in comparison to the Navier-Stokes equations. A subclass of differential type fluids namely the second grade fluid has been reported much in the literature. This subclass can predict the normal stress differences even in the steady flows over a rigid boundary. However a third grade fluid is required in order to investigate the shear thinning/thickening effects. This fluid model has been scarcely studied despite of its complex constitutive relationship in comparison to viscous and second grade fluids. The two-dimensional boundary layer flow of a third order fluid over a stretching sheet has been studied by Sajid and Hayat [1]. The analytic solution of the differential system was developed by homotopy analysis method (HAM). Sajid et al. [2] extended the analysis of ref. [1] by incorporating the MHD and

¹Corresponding author Tel.: + 92 51 90855733
E-mail address: meraj_mm@hotmail.com (M. Mustafa)

heat transfer effects. Unsteady flow with heat and mass transfer of a third grade fluid has been discussed by Hayat et al. [3]. Sahoo [4] numerically investigated the Heimenz flow and heat transfer of a third grade fluid. Slip effects on the third grade fluid flow driven by the stretching surface have been addressed by Sahoo and Do [5].

Two-dimensional stagnation-point flow is one of the classical problems in fluid mechanics. This type of flow has been initiated by Heimenz [6]. It describes the fluid motion near the stagnant region of a circular body. The stretched flows in viscous and non-Newtonian fluids have applications in several industrial processes such as cooling of metallic plate in a bath, a polymer sheet extruded continuously from a die etc. The problem of viscous flow due to a stretching surface has been firstly handled by Crane [7]. Kumar [8] recently studied the effects of heat transfer on the steady boundary layer flow over a stretching surface with power law heat flux. Chiam [9] examined the stagnation point flow of viscous fluid towards a linear stretching surface. Stagnation-point flow of power-law fluid over a stretching surface was reported by Mahapatra et al. [10]. They have obtained a numerical solution of the problem by fourth-order Runge Kutta integration technique. Slip effects on the stagnation-point flow of a second grade fluid were examined by Labropulu and Li [11]. The resulting differential system was solved numerically by quasi-linearization technique. Abbas et al. [12] investigated the mixed convection boundary layer flow of an Upper-Convected Maxwell (UCM) fluid towards a stretching sheet. This problem was solved analytically and numerically by homotopy analysis method (HAM) and finite difference scheme respectively. An analytic solution for unsteady stagnation-point flow driven by impulsively rotating disk has been obtained by Hayat and Nawaz [13].

Melting heat transfer has various industrial applications which involve preparation of semi conductor materials, the melting of permafrost and in the solidification of magma flows. The characteristics of melting heat transfer in the laminar flow over a flat plate were analyzed by Epstein and Cho [14]. Recently Ishak et al. [15] discussed the flow over a melting surface with parallel free stream. Influence of melting heat transfer in the boundary layer stagnation-point flow over a stretching surface has been reported by Bachok et al. [16]. Numerical solutions of the resulting problems in refs. [15] and [16] have been obtained by Runge-Kutta Fehlberg method. To the best of our knowledge no investigation regarding the effects of melting heat transfer on the flows of non-Newtonian fluids has been presented. Therefore the present work deals with the flow analysis of third grade fluid in this direction. The analytic solutions are computed by HAM which has been employed to obtain the solutions of several nonlinear problems [17 – 33]. The solution expressions have been displayed and analyzed.

2. Mathematical formulation

We consider the steady incompressible flow of a third grade fluid near a stagnation-point past stretching sheet situated at $y = 0$, melting at a steady rate into a constant property. We have

taken x - and y - axes along and perpendicular to the sheet, respectively, and the flow is confined to $y \geq 0$. It is assumed that the velocity of the stagnation-point flow is $u_e(x) = ax$ and the velocity of the stretching sheet is $u_w(x) = cx$, where a is a positive constant, while c is a positive (stretching sheet) constant. We have chosen $T_\infty > T_m$ where T_m is the temperature of the melting surface and T_∞ is the ambient temperature. We incorporate the viscous dissipation effects in the energy equation. The boundary layer equations governing the flow and heat transfer of a third grade fluid are [1–5]

$$\frac{\partial u}{\partial x} + \frac{\partial v}{\partial y} = 0, \quad (1)$$

$$\begin{aligned} u \frac{\partial u}{\partial x} + v \frac{\partial u}{\partial y} = & u_e \frac{du_e}{dx} + v \frac{\partial^2 u}{\partial y^2} + \frac{\alpha_1}{\rho} \left[u \frac{\partial^3 u}{\partial x \partial y^2} + v \frac{\partial^3 u}{\partial y^3} + \frac{\partial u}{\partial x} \frac{\partial^2 u}{\partial y^2} + 3 \frac{\partial u}{\partial y} \frac{\partial^2 u}{\partial x \partial y} \right] \\ & + 2 \frac{\alpha_2}{\rho} \frac{\partial u}{\partial y} \frac{\partial^2 u}{\partial x \partial y} + 6 \frac{\beta_3}{\rho} \left(\frac{\partial u}{\partial y} \right)^2 \frac{\partial^2 u}{\partial y^2}, \end{aligned} \quad (2)$$

$$\begin{aligned} u \frac{\partial T}{\partial x} + v \frac{\partial T}{\partial y} = & \alpha \frac{\partial^2 T}{\partial y^2} + \frac{\nu}{C_p} \left(\frac{\partial u}{\partial y} \right)^2 + \frac{\alpha_1}{\rho C_p} \left(u \frac{\partial u}{\partial y} \frac{\partial^2 u}{\partial x \partial y} + v \frac{\partial u}{\partial y} \frac{\partial^2 u}{\partial y^2} \right) \\ & + \frac{2\beta_3}{\rho C_p} \left(\frac{\partial u}{\partial y} \right)^4. \end{aligned} \quad (3)$$

In the above equations u and v are the velocity components along the x - and y - directions respectively, $\alpha_i (i=1,2)$ and β_3 are the material fluid parameters, T is the temperature of the fluid, ν is the kinematic viscosity and α is the thermal diffusivity and C_p is the specific heat of the fluid. The appropriate boundary conditions for the problem are [14]

$$u = u_w(x) = cx, T = T_m \text{ at } y = 0, \quad (4)$$

$$u \rightarrow u_e(x) = ax, T \rightarrow T_\infty \text{ as } y \rightarrow \infty, \quad (5)$$

and

$$k \left(\frac{\partial T}{\partial y} \right)_{y=0} = \rho [\lambda + c_s (T_m - T_0)] v(x, 0) \quad (6)$$

where ρ is the fluid density, k is the thermal conductivity, λ is the latent heat of the fluid and c_s is the heat capacity of the solid surface. The boundary condition (6) shows that the heat conducted to the melting surface is equal to the heat of melting plus the sensible heat required to raise the solid temperature T_0 to its melting temperature T_m (see Epstein and Cho [14]).

We look for a solution of Eqs. (1)–(3) of the form

$$\psi = x\sqrt{c\nu} f(\eta), u = cx f'(\eta), v = -\sqrt{c\nu} f(\eta), \theta(\eta) = (T - T_m)/(T_\infty - T_m), \eta = \sqrt{\frac{c}{\nu}} y, \quad (7)$$

Substituting Eq. (7) into Eqs. (2) and (3), we get the following ordinary differential equations

$$f''' - f'^2 + ff'' + \varepsilon_1(2ff''' - ff'''') + (3\varepsilon_1 + 2\varepsilon_2)f''^2 + 6\phi\phi_1 f''f''^2 + A^2 = 0, \quad (8)$$

$$\theta'' + \text{Pr} f\theta' + \text{Pr} Ec[f''^2 + \varepsilon_1(ff''^2 - ff''f''') + 2\phi\phi_1 f''^4] = 0, \quad (9)$$

where primes denote differentiation with respect to η , Pr is the Prandtl number, ε_1 and ε_2 are the material fluid parameters, ϕ is the third grade fluid parameter, ϕ_1 is the local Reynolds number and Ec is the local Eckert number. These quantities are defined as

$$\begin{aligned} \varepsilon_1 &= \frac{c\alpha_1}{\mu}, \varepsilon_2 = \frac{c\alpha_2}{\mu}, \phi = \frac{c^2\beta_3}{\mu}, \\ \phi_1 &= \frac{cx^2}{\nu}, \text{Pr} = \frac{\nu}{\alpha}, Ec = \frac{u_w^2}{C_p(T_\infty - T_m)}. \end{aligned} \quad (10)$$

The boundary conditions (4) - (6) become

$$\begin{aligned} f'(0) &= 1, \text{Pr} f(0) + M\theta'(0) = 0, \theta(0) = 0, \\ f'(\infty) &= A, f''(\infty) = 0, \theta(\infty) = 1, \end{aligned} \quad (11)$$

where $A = a/c$ is the stretching parameter and M as the dimensionless melting parameter

$$M = \frac{C_p(T_\infty - T_m)}{\lambda + c_s(T_m - T_0)} \quad (12)$$

is a combination of the Stefan numbers $C_p(T_\infty - T_m)/\lambda$ and $c_s(T_m - T_0)/\lambda$ for the liquid and solid phases, respectively. It is noticed that when $\phi = 0$ and $\varepsilon_2 = -\varepsilon_1$ we obtain the governing equations for a second grade fluid. However when $\varepsilon_1 = \varepsilon_2 = \phi = 0$ the governing equations for viscous fluid are recovered. It is noticeable that $Ec = 0$ characterizes that viscous dissipation effects are negligible. It is worth mentioning that for $M = 0$ (melting is absent), Eq. (8) reduces to the classical problem first developed by Hiemenz [6].

The skin friction coefficient C_f and the local Nusselt number Nu_x can be defined as

$$C_f = \frac{\tau_w}{\rho u_w^2}, Nu_x = \frac{xq_w}{k(T_\infty - T_m)}, \quad (13)$$

in which the wall skin friction (τ_w) and the wall heat flux (q_w) are

$$\begin{aligned} \tau_w &= \left[\mu \frac{\partial u}{\partial y} + \alpha_1 \left(u \frac{\partial^2 u}{\partial x \partial y} + 2 \frac{\partial u}{\partial x} \frac{\partial u}{\partial y} + \nu \frac{\partial^2 u}{\partial y^2} \right) + 2\beta_3 \left(\frac{\partial u}{\partial y} \right)^3 \right]_{y=0}, \\ q_w &= -k \left(\frac{\partial T}{\partial y} \right)_{y=0}, \end{aligned} \quad (14)$$

Due to Eqs. (13) and (14) we finally have

$$\begin{aligned} C_f \text{Re}_x^{1/2} &= \left[f'' + \varepsilon_1(3ff'' - ff''') + 2\phi\phi_1 f''^3 \right]_{\eta=0}, \\ Nu_x / \text{Re}_x^{1/2} &= -\theta'(0). \end{aligned} \quad (15)$$

3. Solutions by homotopy analysis method

3.1. Zeroth-order deformation problems

To derive homotopy solutions, we express the velocity and temperature distributions by a set of base functions

$$\{\eta^k \exp(-n\eta) \mid k \geq 0, n \geq 0\} \quad (16)$$

with

$$\begin{aligned} f_m(\eta) &= \sum_{n=0}^{\infty} \sum_{k=0}^{\infty} a_{m,n}^k \eta^k \exp(-n\eta), \\ \theta_m(\eta) &= \sum_{n=0}^{\infty} \sum_{k=0}^{\infty} b_{m,n}^k \eta^k \exp(-n\eta), \end{aligned} \quad (17)$$

in which $a_{m,n}^k$ and $b_{m,n}^k$ are the coefficients .

Based on the rule of solution expression and the boundary conditions (4)-(6) we have selected the following initial guesses $f_0(\eta)$ and $\theta_0(\eta)$ and the linear operators \mathbf{L}_1 and \mathbf{L}_2 (see Liao [17])

$$\begin{aligned} f_0(\eta) &= A\eta + (1-A)(1 - \exp(-\eta)) - \frac{M}{\text{Pr}}, \\ \theta_0(\eta) &= 1 - \exp(-\eta), \end{aligned} \quad (18)$$

$$\begin{aligned} \mathbf{L}_1(f) &= f''' - f', \\ \mathbf{L}_2(f) &= f'' - f, \end{aligned} \quad (19)$$

with

$$\begin{aligned} \mathbf{L}_1[C_1 + C_2 \exp(\eta) + C_3 \exp(-\eta)] &= 0, \\ \mathbf{L}_2[C_4 \exp(\eta) + C_5 \exp(-\eta)] &= 0, \end{aligned} \quad (20)$$

and $C_1 - C_5$ are the constants. With Eqs. (8) and (9) , the definitions of operators \mathbf{N}_1 and \mathbf{N}_2 can be introduced as

$$\begin{aligned} \mathbf{N}_1[\bar{f}(\eta, p)] &= \frac{\partial^3 \bar{f}(\eta, p)}{\partial \eta^3} - \left(\frac{\partial \bar{f}(\eta, p)}{\partial \eta} \right)^2 + \bar{f}(\eta, p) \frac{\partial^2 \bar{f}(\eta, p)}{\partial \eta^2} + A^2 + 6\phi\phi_1 \left(\frac{\partial^2 \bar{f}(\eta, p)}{\partial \eta^2} \right)^2 \frac{\partial^3 \bar{f}(\eta, p)}{\partial \eta^3} \\ &+ \varepsilon_1 \left(2 \frac{\partial \bar{f}(\eta, p)}{\partial \eta} \frac{\partial^3 \bar{f}(\eta, p)}{\partial \eta^3} - \bar{f}(\eta, p) \frac{\partial^4 \bar{f}(\eta, p)}{\partial \eta^4} \right) + (3\varepsilon_1 + 2\varepsilon_2) \left(\frac{\partial^2 \bar{f}(\eta, p)}{\partial \eta^2} \right)^2 \end{aligned} \quad (21)$$

$$\begin{aligned} \mathbf{N}_2[\bar{f}(\eta, p), \tilde{\theta}(\eta, p)] &= \tilde{\theta}''(\eta, p) + \text{Pr} \tilde{\theta}'(\eta, p) \bar{f}(\eta, p) \\ &+ \text{Pr} Ec \left[\begin{aligned} &\left(\frac{\partial^2 \bar{f}(\eta, p)}{\partial \eta^2} \right)^2 + 2\phi\phi_1 \left(\frac{\partial^2 \bar{f}(\eta, p)}{\partial \eta^2} \right)^4 \\ &+ \varepsilon_1 \left\{ \frac{\partial \bar{f}(\eta, p)}{\partial \eta} \left(\frac{\partial^2 \bar{f}(\eta, p)}{\partial \eta^2} \right)^2 - \bar{f}(\eta, p) \frac{\partial^2 \bar{f}(\eta, p)}{\partial \eta^2} \frac{\partial^3 \bar{f}(\eta, p)}{\partial \eta^3} \right\} \end{aligned} \right]. \end{aligned} \quad (22)$$

The problems subjected to zeroth order are

$$(1-p)\mathbf{L}_1[\bar{f}(\eta, p) - f_0(\eta)] = p\hbar_f \mathbf{N}_1[\bar{f}(\eta, p)], \quad (23)$$

$$(1-p)\mathbf{L}_2[\tilde{\theta}(\eta, p) - \theta_0(\eta)] = p \hbar_\theta \mathbf{N}_2[\tilde{\theta}(\eta, p)], \quad (24)$$

$$\begin{aligned} \Pr \bar{f}(0, p) + M\tilde{\theta}'(0, p) = 0, \quad \bar{f}'(0, p) = 1, \quad \bar{f}'(\infty, p) = A, \\ \tilde{\theta}(0, p) = 0, \quad \tilde{\theta}(\infty, p) = 1, \end{aligned} \quad (25)$$

in which \hbar_f and \hbar_θ are the nonzero auxiliary parameters and for $p=0$ and $p=1$, we have

$$\begin{aligned} \bar{f}(\eta, 0) = f_0(\eta), \quad \bar{f}(\eta, 1) = f(\eta), \\ \tilde{\theta}(\eta, 0) = \theta_0(\eta), \quad \tilde{\theta}(\eta, 1) = \theta(\eta). \end{aligned} \quad (26)$$

and $f_0(\eta)$ and $\theta_0(\eta)$ approach $f(\eta)$ and $\theta(\eta)$ respectively, when p has variation from 0 to 1. In view of Taylors' series, one can express that

$$\bar{f}(\eta, p) = f_0(\eta) + \sum_{m=1}^{\infty} f_m(\eta) p^m, \quad f_m(\eta) = \left. \frac{1}{m!} \frac{\partial^m \bar{f}(\eta, p)}{\partial p^m} \right|_{p=0}, \quad (27)$$

$$\tilde{\theta}(\eta, p) = \theta_0(\eta) + \sum_{m=1}^{\infty} \theta_m(\eta) p^m, \quad \theta_m(\eta) = \left. \frac{1}{m!} \frac{\partial^m \tilde{\theta}(\eta, p)}{\partial p^m} \right|_{p=0}. \quad (28)$$

and the convergence of the series (27) and (28) strictly depends upon \hbar_f and \hbar_θ . The values of \hbar_f and \hbar_θ are selected in such a manner that the series (27) and (28) are convergent at $p=1$ and hence Eq. (26) yields

$$f(\eta) = f_0(\eta) + \sum_{m=1}^{\infty} f_m(\eta), \quad (29)$$

$$\theta(\eta) = \theta_0(\eta) + \sum_{m=1}^{\infty} \theta_m(\eta). \quad (30)$$

3.2. m th order deformation problems

At this order, the problems are of the following types

$$\mathbf{L}_1[f_m(\eta, p) - \chi_m f_{m-1}(\eta)] = \hbar_f \mathbf{R}_{1,m}(\eta), \quad (31)$$

$$\mathbf{L}_2[\theta_m(\eta, p) - \chi_m \theta_{m-1}(\eta)] = \hbar_\theta \mathbf{R}_{2,m}(\eta), \quad (32)$$

$$\Pr f_m(0) + M\theta'_m(0) = f'_m(0) = f'_m(\infty) = \theta_m(0) = \theta_m(\infty) = 0, \quad (33)$$

$$\chi_m = \begin{cases} 0, & m \leq 1 \\ 1, & m > 1 \end{cases} \quad (34)$$

$$\begin{aligned} \mathbf{R}_{1,m}(\eta) &= f_{m-1}''' - f_{m-1}'^2 + \sum_{k=0}^{m-1} f_{m-1-k} f_k'' + \varepsilon_1 \sum_{k=0}^{m-1} (2f_{m-1-k}' f_k''' - f_{m-1-k} f_k'''') \\ &+ (3\varepsilon_1 + 2\varepsilon_2) \sum_{k=0}^{m-1} f_{m-1-k}'' f_k'' + 6\phi\phi_1 \sum_{k=0}^{m-1} f_{m-1-k}''' \sum_{l=0}^k f_{k-l}'' f_l'' + A^2(1 - \chi_m), \end{aligned} \quad (35)$$

$$\begin{aligned} \mathbf{R}_{2,m}(\eta) &= \theta_{m-1}'' + \sum_{k=0}^{m-1} \Pr f_{m-1-k} \theta_k' + 2\Pr Ec\phi\phi_1 \sum_{k=0}^{m-1} f_{m-1-k}'' \sum_{l=0}^k f_{k-l}'' \sum_{j=0}^l f_{j-l}'' f_j'' \\ &+ \Pr Ec \sum_{k=0}^{m-1} \left[f_{m-1-k}'' f_k'' + \varepsilon_1 \left(f_{m-1-k}' \sum_{l=0}^k f_{k-l}'' f_l'' - f_{m-1-k} \sum_{l=0}^k f_{k-l}'' f_l''' \right) \right]. \end{aligned} \quad (36)$$

We have used the symbolic computation software MATHEMATICA for the solution of Eqs. (31)-(36). For instance the first order solutions for f and θ are as under:

$$\begin{aligned} f_1 &= \frac{1}{180 \Pr} (e^{-3\eta} (15(-1+A)h_f (3e^{2\eta} (2M(-1+e^\eta - \eta) + A \Pr(5-5e^\eta + \eta(5+\eta))) \\ &+ e^\eta (-8(-1+A) \Pr + e^\eta ((-22+A) \Pr + 7(2+A)e^\eta \Pr + M(6-6e^\eta + 6\eta) - 3\Pr \eta(2+A(5+\eta)))))) \varepsilon_1 \\ &+ (-1+A)(-1+e^\eta)^2 \Pr(-4e^\eta \varepsilon_2 + 3(-1+A)(1+2e^\eta)\phi\phi_1) + e^{2\eta} (180(-1+A) \Pr \\ &+ e^\eta (180(-M + \Pr - A \Pr + A \Pr \eta) + Mh_\theta(-90(1+M) + 15(2+A) \Pr \\ &+ 20(-1+A)^2 Ec(-3M + (3+A) \Pr) \varepsilon_1 + 72(-1+A)^4 Ec \Pr \phi\phi_1))), \end{aligned} \quad (37)$$

$$\begin{aligned} \theta_1 &= \frac{1}{180} e^{-4\eta} (180e^{3\eta} (-1+e^\eta) + h_\theta 15e^{2\eta} (4(A-1)\Pr + e^\eta (6(1+M)\eta \\ &+ \Pr(4-6\eta + A(-4-3(-1+\eta)\eta)))) + 20(-1+A)^2 e^{2\eta} Ec(3(-1+e^\eta)M \\ &+ \Pr(3+4A - (3+4A)e^\eta + 3A\eta)) \varepsilon_1 - 24(-1+A)^4 (-1+e^{3\eta}) Ec \Pr \phi\phi_1). \end{aligned} \quad (38)$$

4. Analysis of the results

4.1 Convergence of the derived series solutions

The series solutions (29) and (30) contain auxiliary parameters h_f and h_θ . The convergence of the obtained series solutions strictly depends upon these parameters (see Liao [17]). In order to obtain the permissible values of auxiliary parameters, the h -curves are sketched at 15th-order of approximations in Fig.1. It is found that range for admissible values of h_f and h_θ are $-1.50 \leq h_f \leq -0.25$ and $-1.25 \leq h_\theta \leq -0.25$. It is noticed that the series solutions converge in the whole region of η ($0 < \eta < \infty$) for $h_f = h_\theta = -0.7$.

4.2 Results and discussion

This section presents the effects of various parameters on the velocity, temperature, skin friction coefficient and local Nusselt number in the form of graphical and tabulated results (see Figs. 2–10 and Table 2 & 3). In order to validate the accuracy of our analytic results, we have given a

comparative study of present HAM solutions with the existing numerical results. The results are in very good agreement (as can be seen from Table 2). Fig.2 displays the velocity profiles for different values of stretching ratio A . The velocity and the boundary layer thickness are decreasing functions of A ($0 \leq A < 1$). However, when free stream velocity dominates the stretching sheet velocity i.e. $A > 1$ the velocity increases and the boundary layer thickness decreases with an increase in A . Fig.3 illustrates the influence of melting parameter M on the velocity f' . An increase in the melting parameter M enhances the velocity and the boundary layer thickness. When a cold sheet plunges into a hot water it starts to melt. As the melting progresses the sheet gradually transforms to a liquid causing the velocity profiles to grow rapidly. The effects of fluid parameters ε_1 and ε_2 on the velocity field f' are depicted in the Figs. 4 and 5. An increase in the values of ε_1 and ε_2 significantly increases the velocity profile f' . It is evident that increase in ε_1 and ε_2 correspond to an increase in the normal stress differences which increase the velocity of fluid. The effect of third grade fluid parameter ϕ is seen in Fig. 6. It is quite obvious from the Fig. 6 that an increase in ϕ corresponds to an increase in the velocity and the boundary layer thickness. From the physical point of view the larger values of ϕ strengthen the shear thinning effect which leads to a decrement in the fluid's viscosity with an increased rate of shear stress which, therefore, causes an increase in the velocity and the boundary layer thickness. The consequences of an increase in Prandtl number Pr on the velocity are visualized in Fig. 7. It is seen that the velocity and the boundary layer thickness are decreasing functions of Pr . Figs. 8–11 analyze the influences of all the parameters on the dimensionless temperature $\theta(\eta)$. An increase in the free stream velocity enhances the temperature and the thermal boundary layer thickness. Figs. 9 and 10 have been portrayed to investigate the effects of fluid parameters ε_1 and ε_2 on the temperature $\theta(\eta)$. The large values of ε_1 and ε_2 accompany with higher normal stress differences which increases the temperature. The influence of melting parameter M on the temperature $\theta(\eta)$ is captured in Fig. 11. It is obvious from this Fig. that an increase in the melting effect decreases the temperature. However, the thermal boundary layer thickness is increased for large values of M . The influence of Prandtl number Pr on the temperature is examined in Fig.12. From the definition of Prandtl number it is quite obvious that a large Prandtl number has a lower thermal diffusivity, therefore an increase in Pr tends to decrease the temperature and thermal boundary layer thickness. Fig.13 captures the effect of Eckert number Ec on the temperature $\theta(\eta)$. The large values of Ec lead to a strong viscous dissipation which appreciably increases the temperature profile.

To ensure the convergence of the obtained homotopy solutions Table 1 is displayed. It is noticed that convergence for the functions f and θ is obtained at only 20th-order of approximations. Table 2 gives the comparison of present series solutions with the numerical results obtained by Ishak et al. [34]. An excellent agreement is found between the two solutions. The numerical values of skin friction coefficient and local Nusselt number for different values of the parameters are computed in Table 3. It is clear that magnitude of skin friction coefficient is an increasing

function of Pr , Ec and ε_1 . However it decreases with an increase in M and ε_2 . The increase in the values of Pr , Ec , ε_1 and ε_2 enhances the magnitude of local Nusselt number. Furthermore it is observed that magnitude of local Nusselt number increases for large values of M .

Table 1: Convergence of the HAM solutions for different order of approximations when $M = 0.5$, $Pr = 1.0$, $A = 0.2$ and $\varepsilon_1 = \varepsilon_2 = \phi = \phi_1 = 0.1$.

Order of approximations	$-f''(0)$	$\theta'(0)$
1	0.677052	0.628970
5	0.743938	0.537406
10	0.743845	0.539327
15	0.743813	0.539457
20	0.743814	0.539455
25	0.743814	0.539455
30	0.743814	0.539455

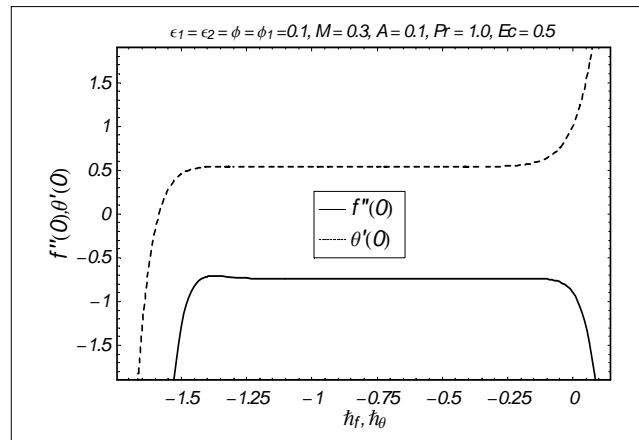


Fig. 1. \tilde{h} –curves for the functions f and θ .

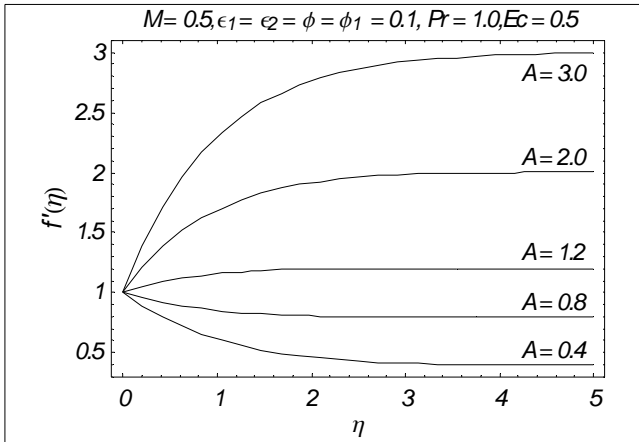


Fig. 2: Influence of A on f' .

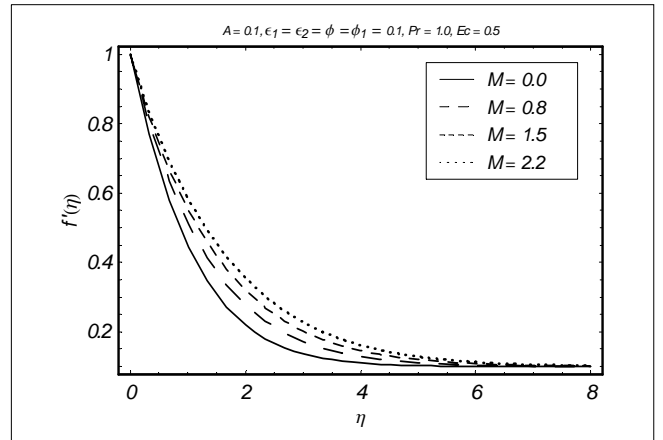


Fig. 3: Influence of M on f' .

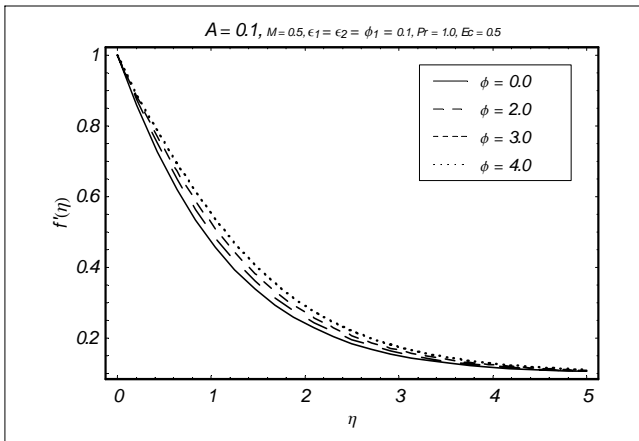


Fig. 4: Influence of ϕ on f' .

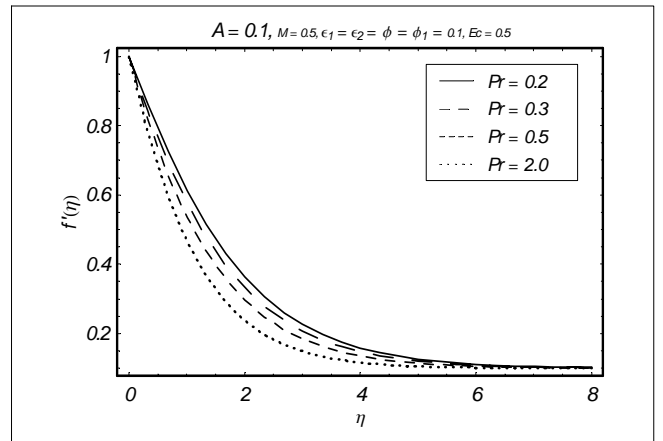


Fig. 5: Influence of Pr on f' .

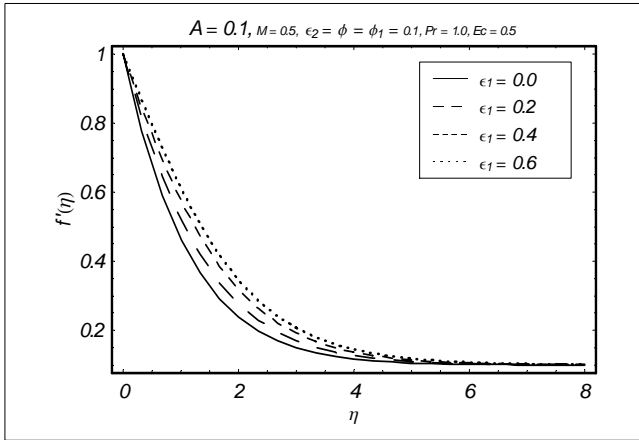


Fig. 6. Influence of ϵ_1 on f' .

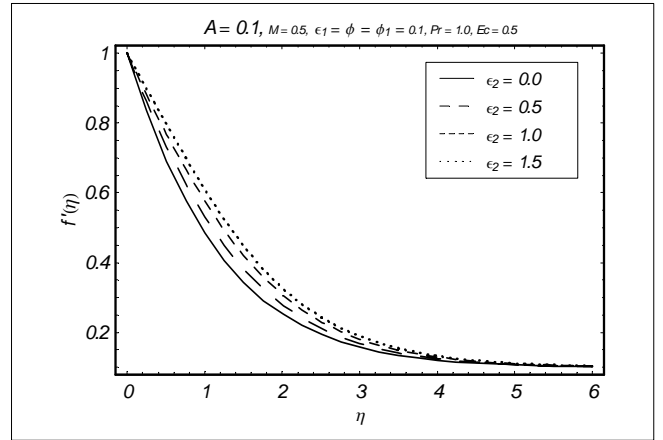


Fig. 7. Influence of ϵ_2 on f' .

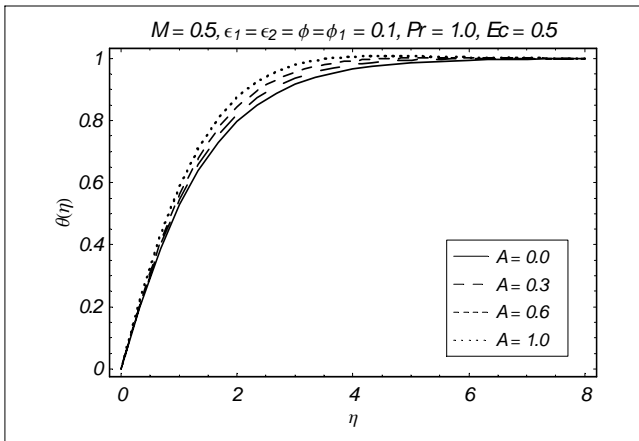


Fig. 8. Influence of A on θ .

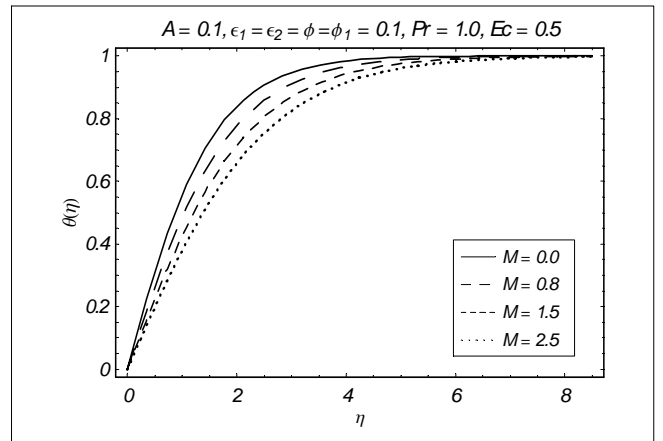


Fig. 9. Influence of M on θ .

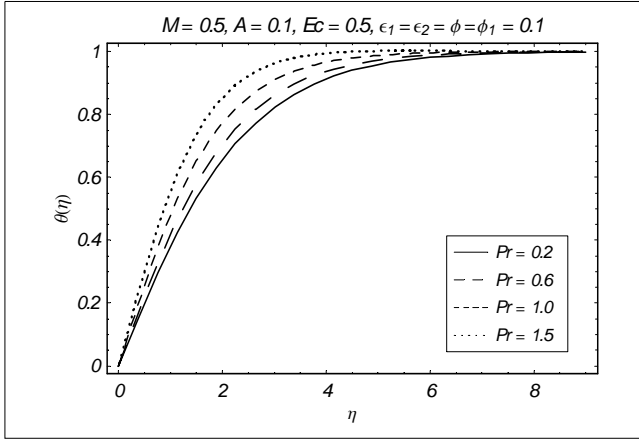


Fig. 10. Influence of Pr on θ .

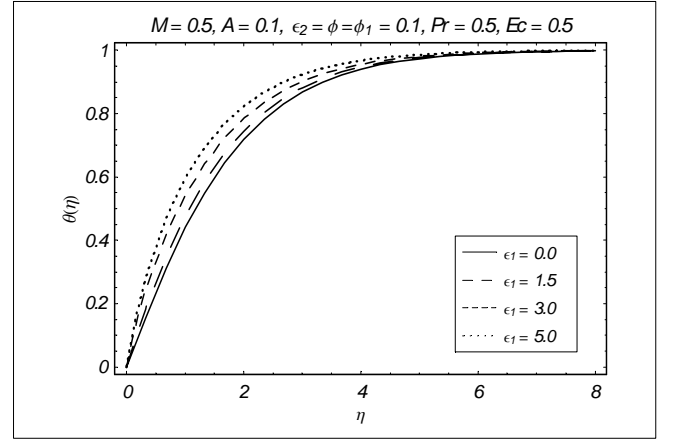


Fig. 11. Influence of ϵ_1 on θ .

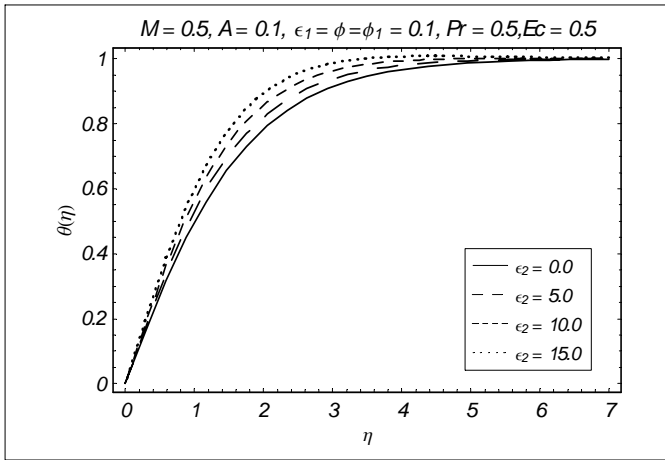


Fig. 12. Influence of ϵ_2 on θ .

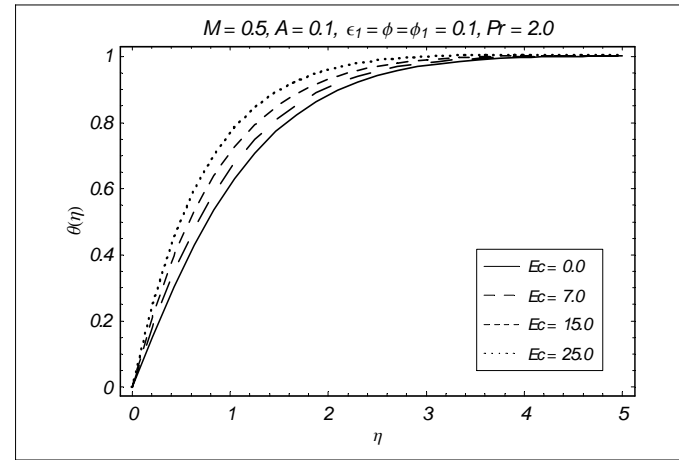


Fig. 13. Influence of Ec on θ .

Table 2: Comparison values of $f''(0)$ with Ishak et al. [34] for various values of A .

A	Present	Ishak et al.[34]
0.01	-0.99801	-0.9980
0.10	-0.96939	-0.9694
0.20	-0.91807	-0.9181
0.50	-0.66735	-0.6673
2.00	2.01767	2.0175
3.00	4.72944	4.7294

Table 3: Values of skin-friction coefficient $R_{e_x}^{1/2} C_f$ and the local Nusselt number $Re_x^{-1/2} Nu_x$ for some values of M , Pr , ϵ_1 and ϵ_2 when $A=0.2$ and $\phi = \phi_1 = 0.1$

M	Pr	ϵ_1	ϵ_2	Ec	$-R_{e_x}^{1/2} C_f$	$-Re_x^{-1/2} Nu_x$
0.0	1.0	0.2	0.2	1.0	1.058180	0.708440
0.3					0.986160	0.588990
0.5					0.951670	0.532610
0.6					0.937069	0.509036
0.5	0.8				0.942859	0.464469
	1.2				0.958661	0.594978
	1.5				0.966706	0.681281
	1.0	0.0			0.749699	0.488358
		0.1			0.855488	0.512659
		0.2			0.951670	0.532610
		0.3			1.040490	0.549368
		0.2	0.0		1.014780	0.529679
			0.1		0.982151	0.529679
			0.2		0.951670	0.532610
			0.3		0.923149	0.534195
			0.2	0.0	0.957020	0.504396
				0.5	0.954325	0.518606
				0.7	0.953244	0.524265

5. Final remarks

In this paper, we have addressed the influence of melting heat transfer on the stagnation-point flow of third grade fluid over a stretching surface. Viscous dissipation effects are present. The analytic solutions have been computed by HAM. The main points of the present study are:

- Table1 ensures that convergence of the functions f and θ are obtained at only 20th-order approximations.
- The behaviors of fluid parameters $\epsilon_i (i=1,2)$ and ϕ on the velocity and boundary layer thickness are similar in a qualitative sense.
- As expected, the effects of melting parameter M and Prandtl number Pr on the velocity and temperature are opposite.

- The influence of stretching ratio A is to increase the velocity and temperature fields significantly.
- The present results are in a very good agreement with the numerical results obtained by Ishak et al. [34] for viscous fluid.

Acknowledgments: We are grateful to the referees for their useful suggestions. Further first author as a visiting Professor thanks the support of Global Research Network for Computational Mathematics and King Saud University of Saudi Arabia.

References

- [1] Sajid, M., Hayat, T., Non-similar series solution for boundary layer flow of a third-order fluid over a stretching sheet, *Appl. Math. Comput.*, 189 (2007), 2, pp. 1576-1585.
- [2] Sajid, M., Hayat, T., Asghar, S., Non-similar analytic solution for MHD flow and heat transfer in a third order fluid over a stretching sheet, *Int. J. Heat Mass Transfer*, 50, 9-10, (2007) 1723-1736.
- [3] Hayat, T., Mustafa, M., Asghar, S., Unsteady flow with heat and mass transfer of a third grade fluid over a stretching surface in the presence of chemical reaction, *Nonlinear Anal : RWA*, 11 (2010), 4, 3186-3197.
- [4] Sahoo, B., Heimenz flow and heat transfer of a third grade fluid, *Comm. Nonlinear Sci. Num. Simul.*, 14 (2009) 811-826.
- [5] Sahoo, B., Do, Y., Effects of slip on sheet driven flow and heat transfer of a third grade fluid pasta stretching sheet, *Int. Comm. Heat Mass Transfer*, 37 (2010), 3, 1064-1071.
- [6] Hiemenz, K., Die Grenzschicht an einem in den gleichförmigen Flüssigkeitsstrom eingetauchten geraden Kreiszyylinder, *Dinglers Polytech. J.*, 326 (1911) 321-324.
- [7] Crane, L. J., Flow past a stretching plate, *Z. Angew. Math. Phys.*, 21 (1970), 4, 645 – 647 .
- [8] H. Kumar, Heat transfer over a stretching porous sheet subjected to power law heat flux in presence of heat source, *Therm. Sci.* doi: 10.2298/TSCI100331074K
- [9] Chiam, T. C., Stagnation-point flow towards a stretching plate, *J. Phys. Soc. Jpn.*, 63 (1994) 2443 – 2444.
- [10] Mahapatra, T. R., Nandy, S. K., Gupta, A. S., Magnetohydrodynamic stagnation-point flow of a power-law fluid towards a stretching surface, *Int. J. Nonlinear. Mech.*, 44(2009), 2, 124 – 129 .
- [11] Labropulu, F., Li, D., Stagnation-point flow of a second grade fluid with slip, *Int. J.*

Nonlinear Mech., 43 (2008), 9, 941–947 .

[12] Hayat, T., Abbas, Z., Sajid, M., MHD stagnation-point flow of an upper-convected Maxwell fluid over a stretching surface, *Chaos Solitons & Fractals*, 39 (2009), 2, 840–848.

[13] Hayat, T., Nawaz, M., Unsteady stagnation point flow of viscous fluid caused by an impulsively rotating disk, *J. Taiwan Inst. Chem. Eng.*, 42 (2011), 1, 41–49 .

[14] Epstein, M., Cho, D. H., Melting heat transfer in steady laminar flow over a flat plate, *J. Heat transfer*, 98 (1976), 3, 531–533 .

[15] Ishak, A., Nazar, R., Bachok, N., Pop, I., Melting heat transfer in steady laminar flow over a moving surface, *Heat Mass Transfer*, 46 (2010), 4, 463–468.

[16] Bachok, N., Ishak, A., Pop, I., Melting heat transfer in boundary layer stagnation-point flow towards a stretching/shrinking sheet, *Phys. Lett. A.*, 374 (2010), 40, 4075–4079 .

[17] Liao, S., Notes on the homotopy analysis method: Some definitions and theorems, *Comm. Nonlinear Sci. Num. Simul.*, 14 (2009), 4, 983–997 .

[18] Liao, S. J., On the relationship between the homotopy analysis method and Euler transform, *Comm. Nonlinear Sci. Numer. Simul.*, 15 (2010), 6, 1421–1431.

[19] Kousar, N., Liao, S. J., Series solution of non-similarity boundary-layer flows over a porous wedge, *Transport in Porous Media*, 83 (2010), 2, 397–412.

[20] Abbasbandy, S., Shivanian, E., Prediction of multiplicity of solutions of nonlinear boundary value problems: Novel application of homotopy analysis method, *Comm. Nonlinear Sci. Num. Simul.*, 15 (2010), 12, 3830–3846.

[21] Abbasbandy, S., Shirzadi, A., A new application of the homotopy analysis method: Solving the Sturm-Liouville problems, *Comm. Nonlinear Sci. Num. Simul.*, 16 (2011), 1, 112–126 .

[22] Hashim, I., Abdulaziz, O., Momani, S., Homotopy analysis method for fractional IVPs, *Comm. Nonlinear Sci. Num. Simul.*, 14 (2009), 3, 674–684.

[23] Bataineh, A. S., Noorani, M. S. M., Hashim, I., On a new reliable modification of homotopy analysis method, *Comm. Nonlinear Sci. Num. Simul.*, 14 (2009), 2, 409–423 .

- [24] Bataineh, A. S., Noorani, M. S. M., Hashim, I., Homotopy analysis method for singular IVPs of Emden--Fowler type, *Comm. Nonlinear Sci. Num. Simul.*, 14(2009), 4, 1121–1131.
- [25] Hayat, T., Qasim, M., Abbas, Z., Homotopy solution for unsteady three-dimensional MHD flow and mass transfer in a porous space, *Comm. Nonlinear. Sci. Num. Simul.*, 15 (2010), 9, 2375–2387.
- [26] Hayat, T., Mustafa, M., Mesloub, S., Mixed convection boundary layer flow over a stretching surface filled with a Maxwell fluid in presence of Soret and Dufour effects, *Z. Naturforsch.*, 65a (2010), 1, 401–410.
- [27] Hayat, T., Mustafa, M., Influence of thermal radiation on the unsteady mixed convection flow of a Jeffrey fluid over a stretching sheet, *Z. Naturforsch.*, 65a (2010), 711–719.
- [28] Hayat, T., Awais, M., Sajid, M., Similar solutions of stretching flow with mass transfer, *Int. J. Num. Meth. Fluids*, 64(2010), 8, 908–921.
- [29] Khan, M., Farooq, J., On heat transfer analysis of a magneto-hydrodynamic Sisko fluid through a porous medium, *J. Porous Media*, 13 (2010), 3, 287-294
- [30] Khan, M., Munawar, S., Abbasbandy, S., Steady flow and heat transfer of a Sisko fluid in annular pipe, *Int. J. Heat Mass Transfer*, 53 (2010), 7-8, 1290-1297.
- [31] Khan, M., Qurrat-ul-Ain, Sajid, M., Heat transfer analysis of the steady flow of an Oldroyd 8-constant fluid due to a suddenly moved plate, *Comm. Nonlinear Sci. Num. Simul.*, 16 (2011), 3, 1347-1355.
- [32] Hayat, T., Shehzad, S. A., Qasim, M., Obaidat, S., Flow of second grade fluid with convective boundary conditions, *Therm. Sci.* doi: 10.2298/TSCI101014058H.
- [33] Ahmad, I., Ahmed, M., Abbas, Z., Sajid, M., Hydromagnetic flow and heat transfer over a bidirectional stretching surface in a porous medium, *Therm. Sci.* doi: 10.2298/TSCI100926006A
- [34] Ishak, A., Nazar, R., Amin, N., Filip, D., Pop, I., Mixed convection in the stagnation point flow towards a stretching vertical permeable sheet, *Malaysian. J. Math. Sci.* 2(2007), 2, 217–226.